Enhancing the transdermal delivery of rigid nanoparticles using the simultaneous application of ultrasound and sodium lauryl sulfate

Renata F.V. Lopez[1,2], **Jennifer E. Seto**[1], **Daniel Blankschtein**[*], and **Robert Langer**
Department of Chemical Engineering, Massachusetts Institute of Technology, Cambridge, MA 02139, USA

Abstract

The potential of rigid nanoparticles to serve as transdermal drug carriers can be greatly enhanced by improving their skin penetration. Therefore, the simultaneous application of ultrasound and sodium lauryl sulfate (referred to as US/SLS) was evaluated as a skin pre-treatment method for enhancing the passive transdermal delivery of nanoparticles. We utilized inductively-coupled plasma mass spectrometry and an improved application of confocal microscopy to compare the delivery of 10- and 20-nm cationic, neutral, and anionic quantum dots (QDs) into US/SLS-treated and untreated pig split-thickness skin. Our findings include: (a) ~0.01% of the QDs penetrate the dermis of untreated skin (which we quantify for the first time), (b) the QDs fully permeate US/SLS-treated skin, (c) the two cationic QDs studied exhibit different extents of skin penetration and dermal clearance, and (d) the QD skin penetration is heterogeneous. We discuss routes of nanoparticle skin penetration and the application of the methods described herein to address conflicting literature reports on nanoparticle skin penetration. We conclude that US/SLS treatment significantly enhances QD transdermal penetration by 500–1300%. Our findings suggest that an optimum surface charge exists for nanoparticle skin penetration, and motivate the application of nanoparticle carriers to US/SLS-treated skin for enhanced transdermal drug delivery.

Keywords

1. Introduction

The evaluation of skin penetration of rigid nanoparticles (e.g. metallic and polymeric) and soft nanoparticles (e.g. liposomes and transfersomes) has recently attracted significant attention [1,2]. In this paper, we focus on rigid nanoparticles. Rigid nanoparticles are being investigated for: (i) designing transdermal drug carriers (e.g. [3,4]), (ii) elucidating their

[*]Corresponding author: Professor Daniel Blankschtein, Massachusetts Institute of Technology, 77 Massachusetts Avenue, Room 66-444, Cambridge, MA 02139, USA, Tel: +1 617 253 4594, Fax: +1 617 252 1651, dblank@mit.edu.
[1]These authors contributed equally to this work.
[2]Permanent address: Department of Pharmaceutical Sciences, School of Pharmaceutical Sciences of Ribeirão Preto, University of São Paulo, Ribeirão Preto, SP 14040-903, Brazil.

mechanism of transdermal penetration (e.g. [5]), and (iii) evaluating their biocompatibility (e.g. [6]). Compared to traditional topical formulation strategies, drug-loaded nanoparticles offer advantages which include protection of unstable active agents against degradation and prolonged release of active agents [2]. In addition, the physicochemical properties of the active agents are masked, and the physicochemical properties of the nanoparticle carrier (e.g. size, surface charge, hydrophilicity, and shape [7–9]) can be designed to enhance the transdermal delivery of the active agent. Furthermore, the nanoparticle carrier can be targeted to deliver the drug to specific skin components, such as dendritic cells [10].

While rigid nanoparticles have potential as transdermal drug carriers, the penetration of nanoparticles into the skin is significantly inhibited by the skin's inherent barrier properties. Many studies have qualitatively shown that skin penetration is primarily limited to the stratum corneum, the outermost skin layer (e.g. [9,11,12]). The ability of nanoparticles to penetrate into the dermis has been debated, based on visual observations made using confocal microscopy (e.g. [7–9,11]). The conflicting reports suggest that nanoparticle penetration into the dermis may occur in very small amounts (e.g. [8]), but this amount has not been quantified previously. Clearly, the success of nanoparticles as transdermal drug carriers depends on the ability of the carrier to penetrate the skin at sufficient depths and in sufficient quantities.

In order to improve nanoparticle skin penetration, one may consider several methods that have been developed to enhance skin permeability [2]. One method, the simultaneous application of low-frequency ultrasound and the surfactant sodium lauryl sulfate (referred to as US/SLS), has received FDA approval as a skin treatment method for enhancing topical lidocaine uptake [13]. US/SLS has also been used to enhance the transdermal delivery of therapeutic macromolecules *in vivo* [14]. To the best of our knowledge, in this paper, we report the first investigation of the application of US/SLS treatment to enhance the passive skin penetration of rigid nanoparticles.

There is significant evidence that the extent of nanoparticle skin penetration depends on the surface charge of the nanoparticle (e.g. [7,9]). Therefore, we compared the penetration of cationic, neutral, and anionic nanoparticles into US/SLS-treated and untreated skin. Quantum dots (QDs) are the nanoparticles selected for this study because: (i) QDs can be coated with various ligands, and therefore, QDs of various surface charges can be obtained, and (ii) their fluorescent properties allow for the visualization of their transdermal route of penetration. More specifically, we compared the following properties of 10- and 20-nm cationic, neutral, and anionic QDs: (a) the penetration of these QDs into US/SLS-treated skin and untreated skin, and (b) the penetration pathway of these nanoparticles. Based on our findings, we draw conclusions regarding the potential of US/SLS as a method to enhance the skin penetration of nanoparticle drug carriers.

2. Materials and methods

2.1 Chemicals

Phosphate buffered saline (PBS) tablets and SLS solution (20 w/v% in water) were obtained from Sigma-Aldrich (St. Louis, MO). PBS was prepared from PBS tablets according to the manufacturer's instructions. NaCl was obtained from Mallinckrodt (Paris, KY). 70% isopropanol wipes were obtained from VWR (West Chester, PA). Deionized water dispensed from a Milli-Q academic water purification system (Millipore, Bedford, MA) was used to prepare solutions. The chemicals used for the ICP-MS analysis (see Section 2.6.1) are provided in ref. [15].

2.2 Quantum dots

Spherical, water soluble, CdSe/ZnS quantum dots with one of three different surface groups were obtained from Ocean NanoTech (Springdale, AR). The surface groups include: (1) cationic polydiallyl dimethyl ammonium chloride, (2) anionic carboxylic acid, and (3) neutral amine. The physicochemical properties of the four QDs studied, referred to hereafter as QDs A D, are listed in Table 1. QD hydrodynamic diameter and ζ potential measurements were performed at 25°C using a ZetaSizer ZS90 (Malvern Instruments, Worcestershire, UK). QD solutions were dialyzed [15] and 0.2-μm filtered prior to analysis. Size measurements were performed at count rates of 100–130 kcps. Sizes were obtained from a volume-based particle size distribution. ζ potentials were measured at the physiologically relevant pHs of 5 and 6 [16]. For ζ potential measurements at pH 6, QDs were dispersed in 10% PBS. For ζ potential measurements at pH 5, QDs were dispersed in 1% PBS, and NaCl was added such that the ionic strength of the solution was equal to that of 10% PBS. ζ potentials were calculated from electrophoretic mobilities using the Smulochowski approximation.

2.3 Skin preparation

The following methods have been described previously [15]. Briefly, 700-μm thick pig split-thickness skin (STS) samples were prepared according to a protocol which was approved by the Committee on Animal Care at MIT. Then, each skin sample was mounted in a Franz diffusion cell (PermeGear, Hellertown, PA) with a 15-mm inner diameter. Any skin sample having an initial electrical resistivity of <50 kΩ cm^2 was considered damaged and was discarded.

We used pig STS, which has minimal variation in dermal thickness, in order to minimize variation in: (1) the amount of QDs quantified in the dermis by ICP-MS (see Section 2.6.1), and (2) the compression of the skin (when it is mounted into an imaging chamber for confocal microscopy analysis; see Section 2.6.2), which affects the observed QD penetration depth. In addition, we have recently shown that pig STS is a convenient skin model for investigating the *in vitro* US/SLS-enhanced transdermal delivery of hydrophilic macromolecules [15], including one of the QDs studied here (QD C).

2.4 US/SLS treatment of skin

US/SLS treatment was applied to some of the skin samples until the desired skin electrical resistivity value of 1.25 ± 0.25 k Ω cm^2 was attained,[3] using a published method [15] which is summarized next: US, with the probe tip immersed in a coupling medium containing 1 w/v% SLS in PBS, was applied to the skin samples with a VCX 500 and a coupler probe (Sonics & Materials, Newtown, CT) at the following typical US conditions [18]: frequency - 20 kHz, intensity - 7.5 W/cm^2, pulse length - 5 seconds on, 5 seconds off, and distance between the probe tip and the skin - 3 mm. The US intensity was calibrated using calorimetry. The US/SLS treatment was stopped at least every minute to determine if the desired skin electrical resistivity value was attained, as well as to replace the coupling medium with a fresh one (to minimize thermal effects).

2.5 Transdermal delivery of QDs

US/SLS-treated and untreated skin samples were mounted into clean, dry Franz diffusion cells. 12 mL of PBS was added to the receiver chambers, and 0.25 mL of 1 μM QD solutions in water was added to the donor chambers. Passive diffusion experiments were conducted for 24 h at room temperature (25°C), and the receiver solutions were

---

[3]This range of skin electrical resistivity values was attained in a US/SLS clinical study [17].

magnetically stirred at 400 RPM. Control experiments were also conducted with water in the donor chamber for: (1) measuring background cadmium (Cd) amounts (recall that Cd is present in the core of the QDs) for ICP-MS analysis (see Section 2.6.1), and (2) configuring confocal microscopy settings (see Section 2.6.2).

2.6 Analysis of QD skin penetration

In *in vitro* transdermal delivery experiments, molecules that permeate the skin are ordinarily quantified in the receiver solution [19]. However, we have previously shown that the dermis acts as a significant diffusion barrier to QDs [15]. Therefore, we analyzed both the receiver solution and the dermis for the presence of QDs.

Immediately following the end of each diffusion experiment, the receiver solution and the skin sample were collected. To prepare the receiver solution for ICP-MS analysis, the receiver solution was dialyzed to reduce the amount of PBS salts [15]. Then, the entire volume of the dialyzed receiver solution was analyzed by ICP-MS. From each skin sample, the skin area that was exposed to US/SLS treatment and subsequent passive application of QDs (1.77 cm^2) was cleaned carefully with isopropanol and PBS and then isolated using scissors. Then, the STS sample was either analyzed by confocal microscopy or further prepared for analysis of QD penetration into the dermis. For the latter analysis, the epidermis was mechanically separated from the dermis using a spatula [15]. Then, the exposed dermal surface was cleaned with isopropanol and PBS in order to minimize potential contamination resulting from inadvertently transferring QDs from the epidermis to the dermis. Finally, the isolated dermis sample was analyzed by either ICP-MS or confocal microscopy as described next.

2.6.1. Quantification of QD penetration by ICP-MS—Inductively coupled plasma-mass spectrometry (ICP-MS) was performed using a PlasmaQuad 2+ Quadrupole Mass Spectrometer (Fisons Instruments, Merrimac, MA) to quantify the amount of ^{111}Cd (an element of the QD core) in the receiver solutions and the dermis samples using a previously published method [15]. The Cd amounts were converted into QD concentrations using calibration plots for each QD studied. It was verified that the skin did not interfere in the quantification of QDs by contacting STS with known concentrations of QDs.

The quantification limit for each type of QD considered (see Table 1) was established as follows: Background Cd amounts were determined using at least three controls (see Section 2.5) in each set of experiments. The maximum amount of Cd found in these controls was doubled; this factor of 2 was chosen to reasonably distinguish between QD and background Cd levels. Using this method, the following quantification limits were determined: (i) 0.007 pmol for QD A, (ii) 0.019 pmol for QD B, (iii) 0.118 pmol for QD C, and (iv) 0.004 pmol for QD D.

For each US/SLS-treated skin sample, the following two quantities were calculated: (1) the total amount of QDs penetrating past the epidermis (the major transdermal diffusion barrier), which corresponds to the sum of the amount of QDs quantified in the dermis and in the receiver chamber, and (2) the fraction of QDs that penetrated past the epidermis and remained in the dermis, which corresponds to the amount of QDs quantified in the dermis divided by (1).

2.6.2. Visualization of QD penetration by confocal microscopy—Within 1–3 hours after the QD skin penetration experiments, STS samples and dermis samples were examined using a LSM 510 confocal microscope, Plan-Neofluar 10x/0.3 objective, and AIM 4.2 software (Carl Zeiss, Jena, Germany). Skin samples were inserted into a 0.5-mm thick imaging chamber (Coverwell PCI-A-0.5, Grace Bio-Labs, Bend, OR) with PBS as the

mounting medium. The imaging chamber was sealed on both sides with a No. 1.5 glass coverslip. Confocal images were obtained in the plane parallel to the sample surface (xy-mode), and optical sections were made in the z-stack mode. All images are 900 μm × 900 μm. Skin samples without QDs were used as negative controls for configuring the microscope settings.

The top surface of the STS samples or of the dermis samples was defined by the scanning depth yielding the highest average fluorescence intensity [5]. After examining the top surface, the samples were turned upside-down, and the underside of the dermis was also examined in search of deep QD penetration into the dermis. As a visual aid, a mark on the coverslip was used to identify the bottom surface of the dermis.

In all figures, a red color scheme is utilized to illustrate routes of QD penetration. In addition, as indicated in the figure captions for Figures 2C, 2D, 3B, 4B, and S2, these images were processed using ImageJ software (National Institutes of Health, Bethesda, MD). The brightness and contrast of the specified images was adjusted first by using the 'Auto' feature in order to enhance the visibility of the regions of QD penetration, and second by increasing the minimum displayed pixel value. These adjustments were propagated to three control images to ensure that the control images remained black. For all images, it is important to recognize that they serve to provide *qualitative* information regarding routes of QD penetration.

2.7 Statistical analysis

Two-sample, two-tailed *t*-tests assuming unequal variances were used to compare QD amounts and ζ potentials. In all analyses, *p* values < 0.05 were considered to be statistically significant.

3. Results

3.1 Quantification of QD penetration into untreated skin

The QDs penetrated into the dermis of untreated skin (see Table 2, Dermis of untreated skin), but QD permeation across the skin and into the receiver chamber of the Franz diffusion cell setup was not quantifiable using ICP-MS (not shown). Among the four QDs, QD C penetrated into the dermis in the largest amounts (0.078% of the applied dose), in spite of the fact that it was not the most cationic QD. QD A penetrated the skin in the smallest amounts (0.006%), in spite of the fact that it was the smallest QD.

3.2 Quantification of QD penetration into US/SLS-treated skin

The US/SLS treatment significantly enhanced the penetration of the QDs past the epidermis (see Table 2, Total) by 500–1300%. In most cases, QDs fully permeated US/SLS-treated skin and reached the receiver chamber in quantifiable amounts (see Table 2, Receiver). QD C penetrated the skin in the largest amounts, while QD A penetrated the skin in the smallest amounts. For all four QDs, the fraction of QDs that penetrated past the epidermis and remained in the dermis was high, ranging from 0.80 to 0.99 (see Table 2, Dermis/Total). Interestingly, the two cationic QDs (C and D) exhibited very different behaviors once they penetrated past the epidermis; out of the four QDs studied, QDs C and D exhibited the smallest and largest fractional retentions in the dermis, respectively.

3.3 Visualization of QD transdermal penetration pathways

Confocal microscopy was used to obtain images of selected skin regions of interest, where QDs penetrated into the stratum corneum and the dermis. These images were used to corroborate the ICP-MS results regarding QD penetration into the dermis and the receiver

chamber. Furthermore, these images provided qualitative information regarding the nature and depth of QD penetration into US/SLS-treated skin and untreated skin. It is important to recognize that the images presented here are regions of interest, in the sense that QD penetration was not observed in the majority of the skin. Instead, QD fluorescence was localized in some hair follicles (see Figure 1) and in regions with diameters typically on the order of 5 μm, but occasionally ranging up to 300 μm for untreated skin and up to 500 μm for US/SLS-treated skin. Furthermore, the regions of QD penetration were generally smaller and observed less frequently in untreated skin compared to those in US/SLS-treated skin.

Figure 2 serves to highlight several aspects of QD transdermal penetration. Based on Figure 2, one can observe that: (1) the intensity of the QD fluorescence in the surface of the stratum corneum (see Figure 2B) and in the section of the dermis at a depth of 25 μm (see Figure 2D) of US/SLS-treated skin are both higher than those of untreated skin (see Figures 2A and 2C, respectively). This corroborates the findings based on ICP-MS that US/SLS treatment of the skin enhances QD penetration into the skin, (2) QDs penetrate into both US/SLS-treated skin and untreated skin in localized regions (i.e. the distribution of QDs in the skin is heterogeneous; see Figure S1), (3) US/SLS treatment increases the fractional surface area of skin through which QD penetration occurs (i.e. the amount of red in Figures 2B and 2D is greater than that in Figures 2A and 2C, respectively), and (4) QDs penetrate into the dermis of untreated skin (see Figure 2C), which provides visual confirmation of the ICP-MS result in Table 2. Observations (1)–(4) were made for all four QDs studied. The number and size of QD penetration regions varied among the QDs, but the discrete nature of QD skin penetration and the increased amount of QD penetration into US/SLS-treated skin compared to that of untreated skin was consistently observed for all four QDs studied.

Both Figures 3 and 4 serve to corroborate the difference in ICP-MS results for the penetration of the cationic QDs into US/SLS-treated skin (see Section 3.2). QD C was observed to penetrate more deeply into the dermis (see the 55.0 μm depth image in Figure 3A). In addition, the QD fluorescence was observed in the bottom layers of the dermis (see Figure 3B). This confirms the uptake of QD C into the deeper portions of the dermis, thus corroborating the ICP-MS analysis which indicated the presence of these QDs in the receiver chamber (see Table 2). On the other hand, while QD D was visually confirmed to penetrate into the dermis, the fluorescence intensity decreased significantly with penetration depth (see Figure 4A). QD D was observed in the bottom layers of US/SLS-treated skin (see Figure 4B). However, these regions of deep dermal penetration were small and difficult to find. Note that only two regions of fluorescence are visible in Figure 4B, while hundreds of small regions of fluorescence are visible in Figure 3B, indicating that QD C was more evenly distributed throughout the bottom layers of the dermis. These observations are consistent with the quantitative findings using ICP-MS which indicated that QD C reached the receiver chamber in greater amounts compared to QD D.

Finally, in untreated skin, QDs were observed to penetrate into the dermis (e.g. see Section S2), but were not observed in the bottom layers of the dermis (not shown). This corroborates the ICP-MS finding that without US/SLS enhancement, QDs did not reach the receiver chambers in quantifiable amounts.

4. Discussion

4.1 QD penetration into untreated skin

The permeation of rigid nanoparticles through untreated skin has previously been investigated (e.g. [3,7–9,11,12]), and conflicting results have been reported. In particular, some research groups claim that observations made using confocal microscopy show no nanoparticle penetration beyond the stratum corneum (SC) of pig STS (e.g. [9,11]). Yet,

others have used confocal microscopy and qualitatively observed nanoparticle penetration into the dermis of pig STS (e.g. [7,8]). In addition, in previous attempts at quantifying nanoparticle skin penetration, no nanoparticles have been detected in the receiver chamber beneath pig STS using either fluorescence measurements or elemental analysis [7,8]. To the best of our knowledge, there have been no previous quantitative reports demonstrating nanoparticle penetration into the dermis of untreated skin.

In the present study, the QDs were not detected to permeate untreated skin to reach the receiver chamber, which is consistent with the previous findings described above. However, the QDs did penetrate the dermis, which we quantified for the first time. Some previous reports have claimed that nanoparticle penetration mainly occurs via hair follicles (e.g. [8,20]). However, we observed QD penetration into the dermis in hair follicles as well as in localized regions outside of hair follicles. To explain this observation, next, we discuss possible routes of passive transdermal penetration of nanoparticles. One commonly proposed route is via aqueous pores located in the head-to-head regions of the SC's lipid matrix [1,7,8,12]. However, the QDs studied here are much larger than the reported average effective aqueous pore diameter of untreated pig STS (3.3 nm [21]). Therefore, QD penetration into the dermis via aqueous pores is unlikely. A more likely route of QD penetration is via lacunar regions (imperfections [22]) present in the lipid bilayers of the SC. The reported mean length of lacunar regions is 183.9 ± 95.03 nm, and the reported mean width is 48.1 ± 12.09 nm [22]. Therefore, the QDs may have permeated across the SC (the major skin diffusion barrier) through these large lacunar regions. However, the area occupied by these imperfections is small (area density, $0.44 \pm 0.11\%$ [22]), leading to the penetration of a very small amount of QDs into the dermis of untreated skin, which was quantifiable by ICP-MS. ICP-MS quantification limits were determined and confocal microscopy was used to visually confirm that the amount of Cd quantified in the dermis cannot be solely attributed to contamination during sample preparation, to leaching of elemental Cd from the QDs, or to background Cd amounts in the skin.

Next, we comment on the conflicting reports in the literature about the ability of nanoparticles to penetrate the dermis of untreated skin. Zhang *et al.* previously stated that the failure to detect nanoparticles in the receiver solution indicates a lack of dermal absorption [8]. However, our combination of quantitative and qualitative results (in addition to previous qualitative results [7]) clearly show that such an analysis is insufficient to determine if nanoparticles can penetrate into the dermis. Furthermore, in the previous applications of confocal microscopy to assess nanoparticle skin penetration, mechanical cross-sections of the skin (i.e. sections made perpendicular to the skin surface) were examined by confocal microscopy (e.g. [7–9,11]). However, since we did not observe nanoparticle penetration in the majority of the skin (i.e. nanoparticle penetration is heterogeneous), we anticipate that many cross-sections of the skin will not contain evidence of deep nanoparticle penetration. In this approach, skin is typically prepared in 20 μm-thick sections, which makes it practically impossible to thoroughly inspect the thousands of sections that can be theoretically produced. Furthermore, since the sectioning knife that creates the cross-sections may inadvertently transfer nanoparticles among the surfaces of the cross-sections, the volume of dermis that can be inspected is reduced, which reduces the probability of observing nanoparticle penetration. All of these reasons explain why this method of sample preparation has yielded inconsistent results. In the present study, we have demonstrated that the nanoparticles studied indeed penetrate the dermis in small, localized regions, which was observed after thorough inspection of the intact dermis that was isolated after nanoparticles were applied to the skin. Therefore, our method of inspecting the isolated, intact dermis for nanoparticle penetration is recommended over inspecting mechanical cross-sections of the skin.

Finally, we highlight additional controversial areas in which our combination of sensitive quantitative and qualitative methods may be applied. First, these methods can be used to address hypotheses based on fluorescence measurements that nanoparticle penetration into human and pig skin may be different, since we have observed that fluorescence measurements alone are insufficient to address this topic (see Section S3). Second, while QDs were utilized as model nanoparticle drug carriers in this work, our results on the ability of nanoparticles to penetrate into the dermis may also be interpreted in the context of nanoparticle toxicity. The exposure of skin to nanoparticles is currently a controversial and sensitive topic because it would have a significant impact on the regulation of several industries, e.g. waste management, cosmetics, and personal care products [23]. Our *in vitro* results indicate that upon applying an aqueous QD solution to skin for 24 h, the QDs have the ability to penetrate into the dermis. However, we caution the interpretation of our results in the context of nanoparticle toxicity. While our results may be concerning because the dermis is the vascularized layer of the skin that can provide access for systemic absorption [7], we note that the exposure of skin to an aqueous solution for 24 hours is an extreme condition. In addition, water is a penetration enhancer [24], and therefore, skin hydration may facilitate QD skin penetration. Nevertheless, we stress that the application of the quantitative and qualitative methods described in the present study may be useful to address some of the conflicting reports in the field of nanoparticle skin toxicity.

4.2 QD penetration into US/SLS-treated skin

The US/SLS skin treatment promoted the permeation of the QDs across the skin into the receiver chamber in significant amounts, which was quantified using ICP-MS (see Table 2) and visually confirmed by using confocal microscopy to observe QDs in the bottom layers of the dermis (see Figures 3B and 4B). In addition, while the majority of the QDs penetrating past the epidermis remained in the dermis, it is important to recognize that, *in vivo*, systemic transdermal drug delivery does not require permeation across the entire dermis layer [25]. Indeed, once the blood capillaries near the epidermis/dermis junction are reached, the drug can be delivered. Our findings suggest that the US/SLS skin treatment represents a viable method to significantly increase the penetration depth and quantity of nanoparticle carriers, thereby enhancing the potential of nanoparticles to serve as useful transdermal drug carriers.

Next, we comment on the extent of transdermal drug delivery enhancement attained with the US/SLS skin treatment. In this study, the amount of QDs penetrating past the epidermis of US/SLS-treated skin ranged from 1/100th to 1/1000th of the amount in the aqueous topical formulation (250 pmol). It is important to recognize that in this study, QDs served as model nanoparticle drug carriers, and the efficacy of the US/SLS-enhanced transdermal delivery method will depend on various factors that are application-specific, e.g. the US/SLS skin treatment parameters, various physicochemical properties of the carriers (including size, charge, hydrophilicity, and shape), the loading of the drug carrier, the drug potency, the amount of drug required for therapeutic effect, and the topical formulation. All of these factors must be considered in order to evaluate the viability of a particular US/SLS-enhanced transdermal drug delivery application.

The ability of the QDs to fully permeate US/SLS-treated skin, and the discrete nature of the QD penetration pathways into US/SLS-treated skin, can be explained by several mechanisms: (1) the US/SLS skin treatment increases the area density, length, and connectivity of the lacunar regions within the SC [22], (2) the US/SLS treatment increases the average effective aqueous pore diameter of pig STS from 3.3 nm [21] to 22.6 nm [15], and (3) the US/SLS treatment enhances skin permeability in a heterogeneous manner. Regarding (3), this phenomenon of heterogeneity in US/SLS-treated skin has been well-documented in pig full-thickness skin (FTS) [18,26]. Specifically, at an US frequency of 20

kHz, the US/SLS treatment creates localized transport regions (LTRs) with a reported average effective aqueous pore diameter of greater than 60 nm [26]. The surrounding regions (referred to as non-LTRs) have a reported average effective aqueous pore diameter of 3.7 nm [26]. Note that untreated pig FTS and STS have similar pore diameters [21], and that US/SLS-treated pig FTS and STS have similar pore diameters [15]. Therefore, it is reasonable to assume that the distribution of LTRs and non-LTRs (and their respective pore diameters) within FTS and STS are similar. Next, we make use of this assumption to discuss our results.

First, in ref. [26], US/SLS treatment was applied to pig FTS to attain three skin electrical resistivity values of 0.8, 0.6, and 0.5 kΩ cm^2. Skin samples treated to 0.8 kΩ cm^2 had an average LTR fractional area of 11%, which varied inversely with skin electrical resistivity [26]. In the present study, skin samples were treated to attain electrical resistivities of 1.25 ± 0.25 kΩ cm^2, which required less US/SLS treatment than that utilized in ref. [26]. Therefore, we can safely over-estimate the fractional area of LTRs in the present study to be 11%. This implies that the non-LTRs occupied at least 90% of each US/SLS-treated skin sample. Since the non-LTRs occupy the majority of the skin, and since the reported non-LTR average pore size (3.7 nm [26]) is much smaller than the size of the QDs studied here, our finding that QD penetration was not observed in the majority of the skin (corresponding to non-LTRs) is reasonable.

Second, the reported LTR pore size of >60 nm [26] explains why the QDs were able to penetrate US/SLS-treated skin in localized regions. The observation of the QDs penetrating the dermis (see Figures 3 and 4) provides visual support to the previously proposed hypothesis that LTRs dominate transdermal transport even in the dermis [27]. As suggested previously, the transformation of LTR formation from a heterogeneous to a homogeneous phenomenon has the potential to further enhance the transdermal penetration of macromolecules [18], including nanoparticles.

4.3 Effect of surface charge on QD transdermal penetration

It has previously been shown that cationic nanoparticles have an affinity for the negatively-charged skin pores, in contrast to anionic nanoparticles, when they are applied to untreated skin [7,9]. Based on these previous findings, one might expect QD D to penetrate skin in greater amounts compared to QDs A–C. However, we have quantitatively and qualitatively demonstrated that among the four QDs studied, the QD that exhibited the greatest ability to penetrate both untreated skin and US/SLS-treated skin was not the most cationic QD. This suggests that there is an optimum cationic surface charge for nanoparticle skin penetration. A nanoparticle that is too cationic may experience hindered diffusion due to strong electrostatic interactions with the negatively-charged skin. Furthermore, the two cationic QDs (C and D) exhibited very different behaviors once they penetrated past the epidermis; out of the four QDs studied, QDs C and D exhibited the smallest and largest fractional retentions in the dermis, respectively. This result was corroborated by Figures 3 and 4, which show that QD C more readily penetrated into the deep layers of the dermis compared to QD D. Therefore, surface charge plays a role in the penetration depth of the nanoparticle. In future studies, one may want to optimize the nanoparticle surface charge such that the nanoparticle drug carrier penetrates the skin at sufficient depths and in sufficient quantities. The desired nanoparticle penetration depth will differ for systemic and topical drug delivery applications. For topical applications, perhaps, a drug carrier's surface charge can be tuned to target specific entities found at different depths within the skin.

Finally, QD A penetrated both untreated skin and US/SLS-treated skin in the smallest amounts, in spite of being smaller than the other QDs. Therefore, our findings strongly suggest that the anionic surface charge is the least favorable for nanoparticle skin

penetration, which is consistent with previous experimental findings [7,9]. In addition, this result is consistent with the theoretical finding that a charged particle diffusing through a pore of like charge will experience reduced mobility compared to a neutral particle of the same size [28]. Because the skin pores are negatively charged, anionic nanoparticles are expected to permeate the skin in smaller amounts compared to neutral ones.

4.4 Outlook

Future studies should be conducted to determine the optimum cationic surface charge for nanoparticle skin penetration. Subsequently, US/SLS treatment followed by the passive application of cationic nanoparticle carriers can be a good strategy, not only for transdermal drug delivery, but also for topical drug delivery and for transcutaneous immunization. The US/SLS-enhanced delivery of a nanoparticle carrier is particularly relevant for transcutaneous immunization. First, a nanoparticle carrier can enhance the delivery of a vaccine to the dendritic cells within skin, and furthermore, the carrier can be targeted to enhance the specific uptake of the vaccine by the dendritic cells [10]. Second, the US/SLS treatment can enhance the immune response induced by simple, naked vaccine application by enhancing the penetration of the vaccine and by acting as an adjuvant [29–31]. Therefore, we propose that the combined application of cationic nanoparticle carriers to US/SLS-treated skin represents an interesting and valuable tool for further developing transcutaneous immunization. Work along these lines is currently in progress.

5. Conclusions

In this study, we demonstrated the use of very sensitive, complementary, quantitative and qualitative methods to evaluate the delivery of nanoparticles into the dermis. These methods will be useful in future assessments of nanoparticle skin penetration. Using ICP-MS, we provided the first quantification of QD penetration into the dermis of untreated skin. In addition, we demonstrated an improved approach to implement confocal microscopy to assess dermal penetration, and we observed that QD skin penetration is heterogeneous. We combined ICP-MS and confocal microscopy to show that the US/SLS skin treatment can significantly enhance the skin penetration of nanoparticles, thereby enhancing the potential of nanoparticles to serve as transdermal drug carriers. Unexpectedly, the QD that exhibited the greatest skin penetration was not the most cationic QD. In addition, the most cationic QD studied exhibited the lowest clearance from the dermis of US/SLS-treated skin. Our findings suggest that an optimum surface charge exists for nanoparticle skin penetration, and motivate the application of nanoparticle carriers to US/SLS-treated skin for enhanced transdermal drug delivery.

Supplementary Material

Refer to Web version on PubMed Central for supplementary material.

Acknowledgments

References

1. Baroli B. Penetration of nanoparticles and nanomaterials in the skin: fiction or reality? J Pharm Sci 2010;99(1):21–50. [PubMed: 19670463]

2. Cevc G, Vierl U. Nanotechnology and the transdermal route: a state of the art review and critical appraisal. J Control Release 2010;141(3):277–99. [PubMed: 19850095]

3. Patlolla RR, Desai PR, Belay K, Singh MS. Translocation of cell penetrating peptide engrafted nanoparticles across skin layers. Biomaterials 2010;31(21):5598–607. [PubMed: 20413152]

4. Lee PW, Hsu SH, Tsai JS, Chen FR, Huang PJ, Ke CJ, et al. Multifunctional core-shell polymeric nanoparticles for transdermal DNA delivery and epidermal Langerhans cells tracking. Biomaterials 2010;31(8):2425–34. [PubMed: 20034662]

5. Kuo TR, Wu CL, Hsu CT, Lo W, Chiang SJ, Lin SJ, et al. Chemical enhancer induced changes in the mechanisms of transdermal delivery of zinc oxide nanoparticles. Biomaterials 2009;30(16): 3002–8. [PubMed: 19232716]

6. Ryman-Rasmussen JP, Riviere JE, Monteiro-Riviere NA. Surface coatings determine cytotoxicity and irritation potential of quantum dot nanoparticles in epidermal keratinocytes. J Invest Dermatol 2007;127:143–53. [PubMed: 16902417]

7. Ryman-Rasmussen JP, Riviere JE, Monteiro-Riviere NA. Penetration of intact skin by quantum dots with diverse physicochemical properties. Toxicol Sci 2006;91(1):159–65. [PubMed: 16443688]

8. Zhang LW, Yu WW, Colvin VL, Monteiro-Riviere NA. Biological interactions of quantum dot nanoparticles in skin and in human epidermal keratinocytes. Toxicol Appl Pharmacol 2008;228(2): 200–11. [PubMed: 18261754]

9. Wu X, Landfester K, Musyanovych A, Guy RH. Disposition of charged nanoparticles after their topical application to the skin. Skin Pharmacol Physiol 2010;23(3):117–23. [PubMed: 20051712]

10. Park K. Nano is better than micro for targeted vaccine delivery. J Controlled Release 2010;144(2): 117.

11. Wu X, Price GJ, Guy RH. Disposition of nanoparticles and an associated lipophilic permeant following topical application to the skin. Mol Pharm 2009;6(5):1441–8. [PubMed: 19630400]

12. Baroli B, Ennas MG, Loffredo F, Isola M, Pinna R, Lopez-Quintela MA. Penetration of metallic nanoparticles in human full-thickness skin. J Invest Dermatol 2007;127(7):1701–12. [PubMed: 17380118]

13. Gupta J, Prausnitz MR. Recovery of skin barrier properties after sonication in human subjects. Ultrasound Med Biol 2009;35(8):1405–8. [PubMed: 19540658]

14. Ogura M, Paliwal S, Mitragotri S. Low-frequency sonophoresis: current status and future prospects. Adv Drug Del Rev 2008;60(10):1218–23.

15. Seto JE, Polat BE, Lopez RFV, Blankschtein D, Langer R. Effects of ultrasound and sodium lauryl sulfate on the transdermal delivery of hydrophilic permeants: comparative in vitro studies with full-thickness and split-thickness pig and human skin. J Controlled Release 2010;145(1):26–32.

16. Matousek JL, Campbell KL. A comparative review of cutaneous pH. Vet Dermatol 2002;13(6): 293–300. [PubMed: 12464061]

17. Farinha A, Kellogg S, Dickinson K, Davison T. Skin impedance reduction for electrophysiology measurements using ultrasonic skin permeation: initial report and comparison to current methods. Biomed Instrum Technol 2006;40(1):72–7. [PubMed: 16544793]

18. Kushner J, Blankschtein D, Langer R. Heterogeneity in skin treated with low-frequency ultrasound. J Pharm Sci 2008;97(10):4119–28. [PubMed: 18240305]

19. Pendlington, RU. In vitro percutaneous absorption measurements. In: Chilcott, RP.; Price, S., editors. Principles and Practice of Skin Toxicology. England: John Wiley & Sons Ltd; 2008. p. 129-48.

20. Alvarez-Román R, Naik A, Kalia YN, Guy RH, Fessi H. Skin penetration and distribution of polymeric nanoparticles. J Control Release 2004;99(1):53–62. [PubMed: 15342180]

21. Polat BE, Seto JE, Blankschtein D, Langer R. Application of the aqueous porous pathway model to quantify the effect of sodium lauryl sulfate on ultrasound-induced skin structural perturbation. J Pharm Sci. (in press). 10.1002/jps.22361

22. Paliwal S, Menon GK, Mitragotri S. Low-frequency sonophoresis: ultrastructural basis for stratum corneum permeability assessed using quantum dots. J Invest Dermatol 2006;126(5):1095–101. [PubMed: 16528354]

23. Monteiro-Riviere, NA.; Baroli, B. Nanomaterial penetration. In: Monteiro-Riviere, NA., editor. Toxicology of the skin. New York: Informa Healthcare; 2010. p. 333-46.

24. Roberts, MS.; Walker, M. Water: the most natural penetration enhancer. In: Walters, KA.; Hadgraft, J., editors. Pharmaceutical skin penetration enhancement. New York: Marcel Dekker, Inc; 1993. p. 1-30.

25. Bronaugh, RL. Methods for in vitro percutaneous absorption. In: Zhai, H.; Wilhelm, K-P.; Maibach, HI., editors. Marzulli and Maibach's Dermatotoxicology. 7. Florida: CRC Press; 2007. p. 307-10.

26. Polat BE, Figueroa PL, Blankschtein D, Langer R. Transport pathways and enhancement mechanisms within localized and non-localized transport regions in skin treated with low-frequency sonophoresis and sodium lauryl sulfate. J Pharm Sci. (in press). 10.1002/jps.22280

27. Tezel A, Sens A, Mitragotri S. A theoretical analysis of low-frequency sonophoresis: dependence of transdermal transport pathways on frequency and energy density. Pharm Res 2002;19(12): 1841–6. [PubMed: 12523663]

28. Dechadilok P, Deen WM. Electrostatic and electrokinetic effects on hindered convection in pores. J Colloid Interface Sci 2009;338(1):135–44. [PubMed: 19589534]

29. Tezel A, Paliwal S, Shen Z, Mitragotri S. Low-frequency ultrasound as a transcutaneous immunization adjuvant. Vaccine 2005;23(29):3800–7. [PubMed: 15893617]

30. Dahlan A, Alpar HO, Stickings P, Sesardic D, Murdan S. Transcutaneous immunisation assisted by low-frequency ultrasound. Int J Pharm 2009;368(1–2):123–8. [PubMed: 19013510]

31. Paliwal S, Mitragotri S. Therapeutic opportunities in biological responses of ultrasound. Ultrasonics 2008;48(4):271–8. [PubMed: 18406440]

Appendix

Full color images and supplementary data and discussions are available in the online version of this article.
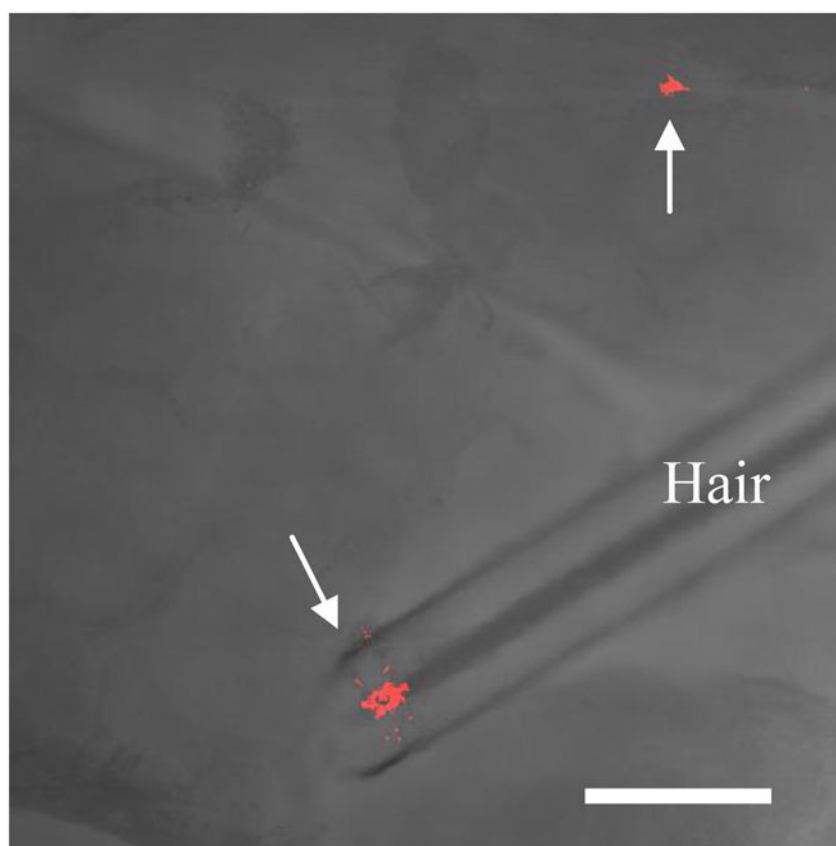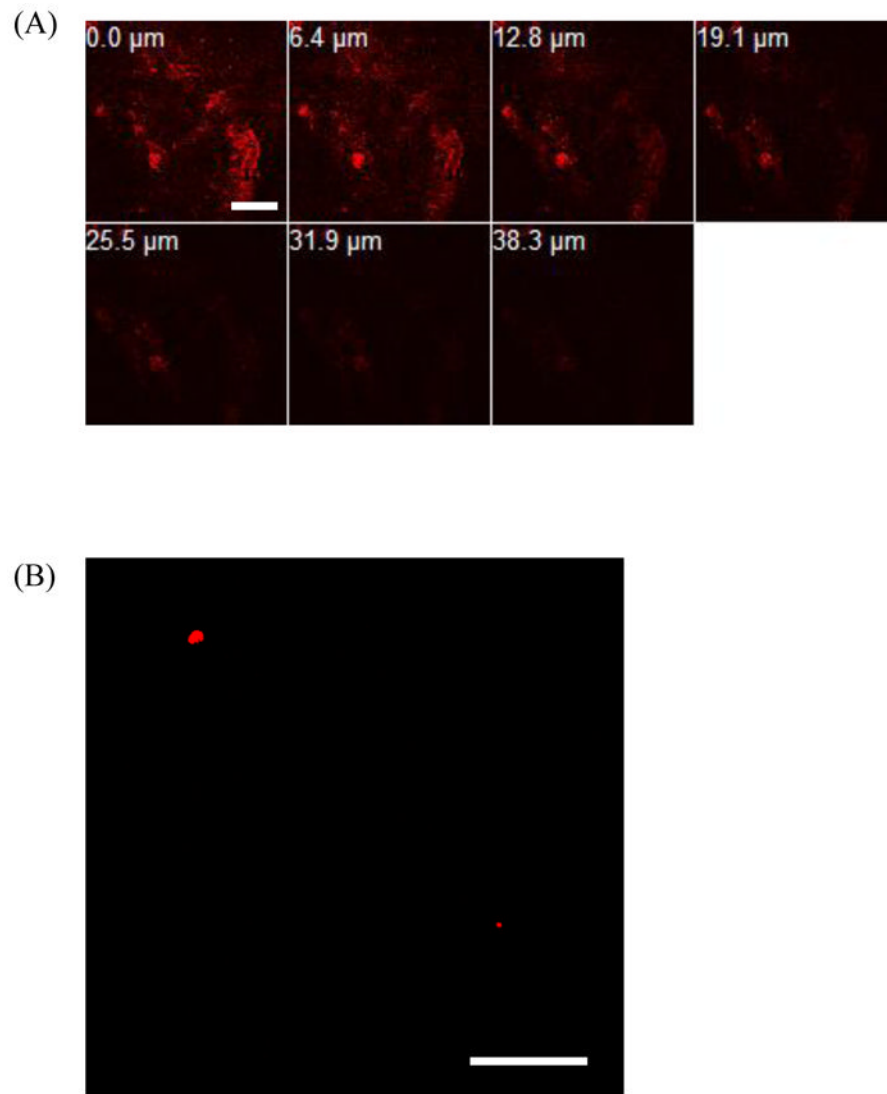
Figure 1.
QD D penetration into US/SLS-treated skin in patches that were not limited to within hair follicles. Optical section of the isolated dermis, made parallel to the epidermis-dermis surface at a depth of 10 μm below the surface. The arrows indicate regions of QD penetration. The image is an overlay of fluorescence and bright-field images. Bar = 200 μm.
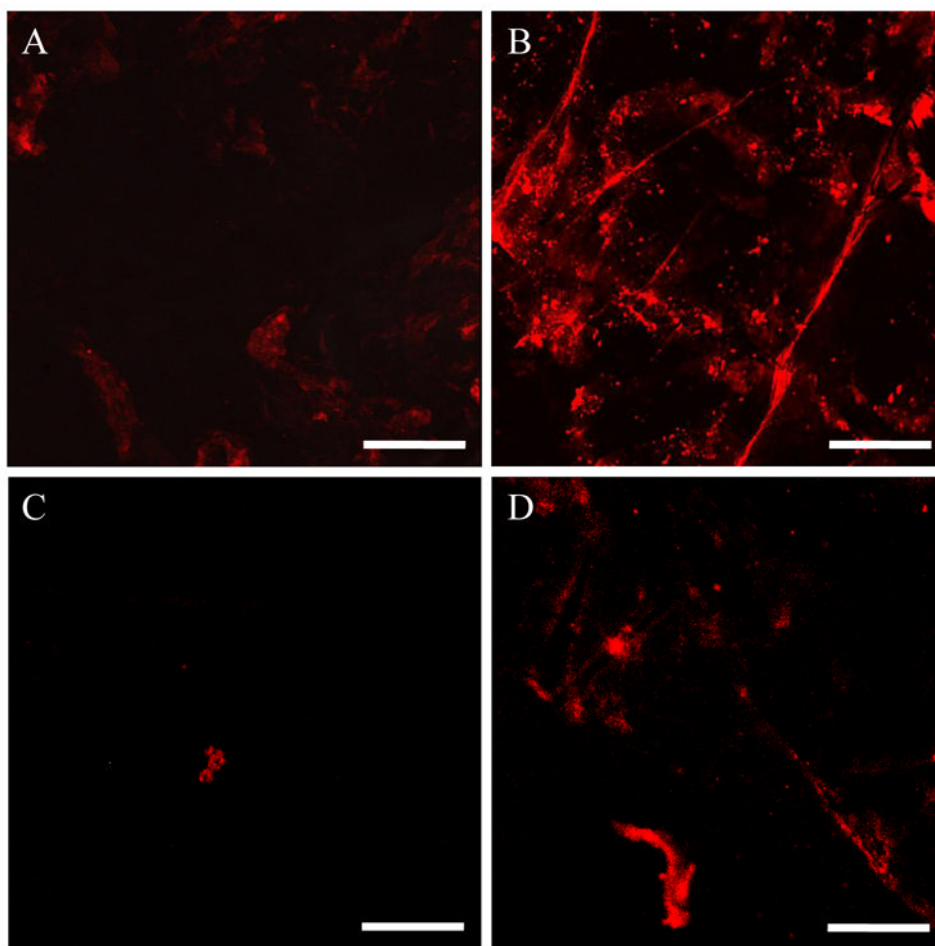
Figure 2.
Confocal images of selected regions of interest in the skin after 24 h of QD penetration into skin. (A) Surface of the stratum corneum (SC) after QD C penetration into untreated skin, (B) Surface of the SC after QD C penetration in US/SLS-treated skin, (C) Optical section of the isolated dermis, made parallel to the epidermis-dermis surface at a depth of 25 μm below the surface, after QD D penetration into untreated skin, and (D) Optical section of the isolated dermis, made to a depth of 25 μm below the surface, after QD D penetration into US/SLS-treated skin. Brightness/contrast enhancement was applied to (C) and (D). Bar = 200 μm.

(A)

(B)
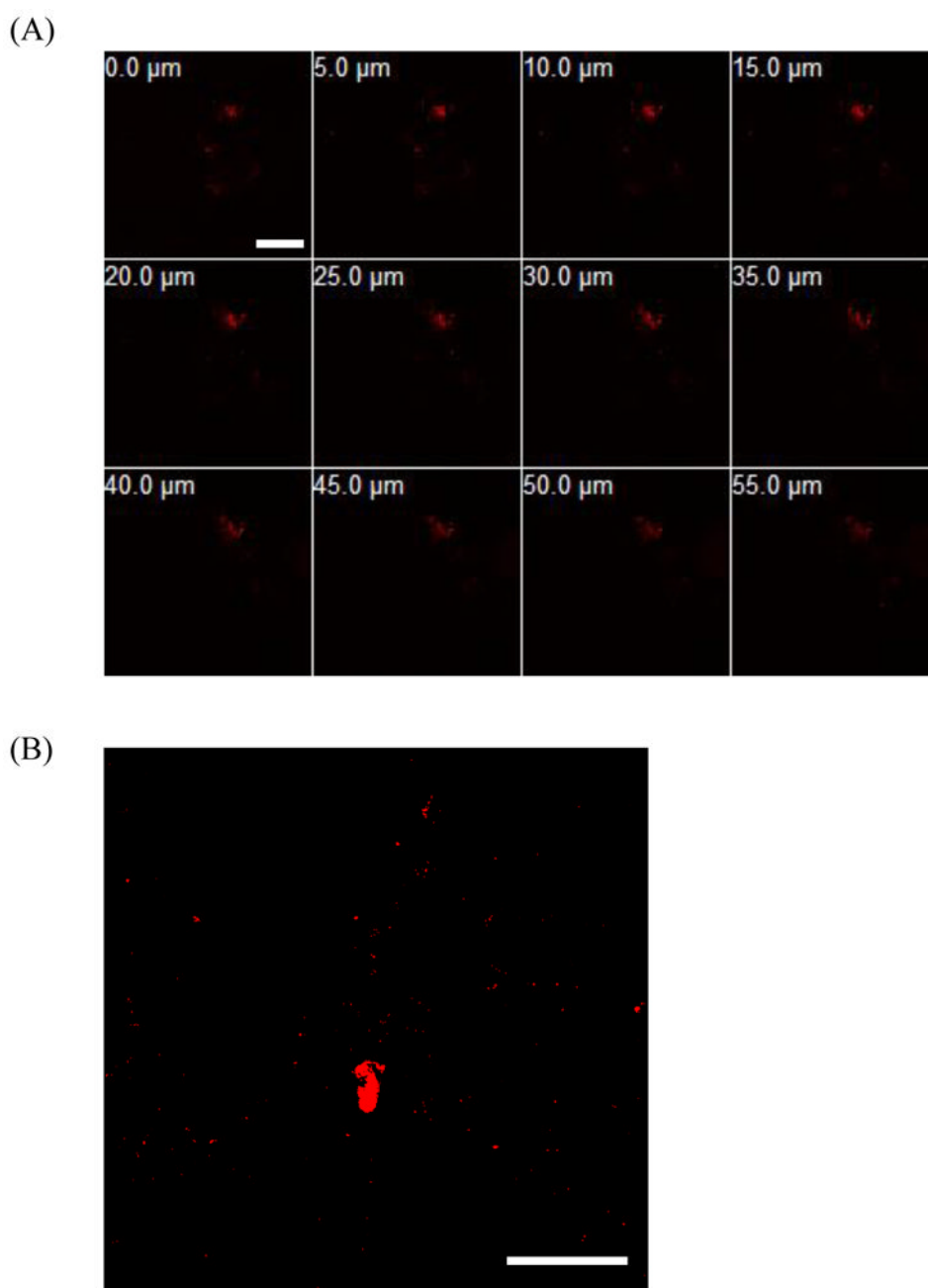
Figure 3.
Confocal images of a selected region of interest in the isolated dermis after 24 h of QD C permeation across US/SLS-treated skin. (A) Optical sections parallel to the top dermis surface (corresponding to 0.0 μm) to a depth of 55.0 μm below the top dermis surface. (B) Optical section from 30 μm above the bottom dermis surface. Brightness/contrast enhancement was applied to (B). Note that the thickness of the dermis is on the order of 600 μm. Bar = 200 μm.

(A)

0.0 µm 6.4 µm 12.8 µm 19.1 µm
25.5 µm 31.9 µm 38.3 µm

(B)

Figure 4.
Confocal images of a selected region of interest in the isolated dermis after 24 h of QD D penetration into US/SLS-treated skin. (A) Optical sections parallel to the top dermis surface (corresponding to 0.0 µm) to a depth of 38.3 µm below the top dermis surface. (B) Optical section from 30 µm above the bottom dermis surface. Brightness/contrast enhancement was applied to (B). Note that the thickness of the dermis is on the order of 600 µm. Bar = 200 µm.

Table 1

Physicochemical properties of the QDs

QD	Hydrodynamic diameter (nm) [b]	ζ potential (mV) at pH 5 [c]	ζ potential (mV) at pH 6 [c]	Classification
A [a]	9.9 ± 0.8	-27.6 ± 3.2	-27.0 ± 1.7	Anionic
B	21.0 ± 0.6	-1.2 ± 0.3	-2.5 ± 3.2	Neutral
C	21.8 ± 1.2	27.6 ± 0.8	26.9 ± 1.3	Cationic
D	21.4 ± 2.0	36.9 ± 1.1 [d]	30.0 ± 1.6 [d]	Cationic

[a] This is the largest anionic QD available from this vendor.

[b] Mean ± SD of 6–9 measurements.

[c] Mean ± SD of 3–6 measurements.

[d] QD D is more cationic than QD C ($p < 0.05$).

Table 2

Quantification of QD skin penetration after 24 h of diffusion. Data shown are the mean ± SD of n replicates; n = 5–6 for US/SLS-treated skin, n = 3–5 for untreated skin

QD	Dermis of untreated skin (pmol)	US/SLS-treated skin			
		Dermis (pmol)	Receiver (pmol)	Total (pmol) [a]	Dermis/Total
A	0.015±0.006	0.115±0.024	0.007±0.006 [b]	0.122±0.025	0.945±0.045
B	0.113±0.055	0.644±0.098	0.044±0.031	0.689±0.095	0.935±0.043
C	0.195±0.055	1.054±0.218	0.244±0.039	1.311±0.239	0.800±0.026
D	0.042±0.021	0.582±0.236	0.006±0.005 [b]	0.587±0.238	0.990±0.006

[a] Total = Dermis + Receiver. These amounts are significantly greater than the QD amounts quantified in the dermis of untreated skin ($p < 0.05$).

[b] In two of the individual skin samples included in this average, the amount of QDs in the receiver chamber was below the quantification limit.